

RESEARCH PAPER

The genetic architecture of branched-chain amino acid accumulation in tomato fruits

Andrej Kochevenko and Alisdair R. Fernie*

Max-Planck-Institute of Molecular Plant Physiology, Am Mühlenberg 1, D-14476 Potsdam-Golm, Germany

* To whom correspondence should be addressed. E-mail: fernie@mpimp-golm.mpg.de

Received 19 January 2011; Revised 2 March 2011; Accepted 3 March 2011

Abstract

Previous studies of the genetic architecture of fruit metabolic composition have allowed us to identify four strongly conserved co-ordinate quantitative trait loci (QTL) for the branched-chain amino acids (BCAAs). This study has been extended here to encompass the other 23 enzymes described to be involved in the pathways of BCAA synthesis and degradation. On coarse mapping the chromosomal location of these enzymes, it was possible to define the map position of 24 genes. Of these genes eight co-localized, or mapped close to BCAA QTL including those encoding ketol-acid reductoisomerase (KARI), dihydroxy-acid dehydratase (DHAD), and isopropylmalate dehydratase (IPMD). Quantitative evaluation of the expression levels of these genes revealed that the *S. pennellii* allele of IPMD demonstrated changes in the expression level of this gene, whereas those of KARI and DHAD were invariant across the genotypes. Whilst the antisense inhibition of IPMD resulted in increased BCAA, the antisense inhibition of neither KARI nor DHAD produced a clear effect in fruit BCAA contents. The results are discussed both with respect to the roles of these specific enzymes within plant amino acid metabolism and within the context of current understanding of the regulation of plant branched-chain amino acid metabolism.

Key words: Branched-chain amino acid, introgression line, metabolic regulation, quantitative trait analysis, reverse genetics, tomato fruit metabolism.

Introduction

Despite the fact that the branched-chain amino acids are essential components of the mammalian diet, our understanding of their metabolism in plants remains far from complete. The synthetic pathways for leucine, isoleucine, and valine are relatively well established (Schulze-Siebert *et al.*, 1984; Hagelstein *et al.*, 1997). Intriguingly, activity of the same set of enzymes of two pathways running in parallel leads to different products, valine and isoleucine. Leucine biosynthesis, however, branches off from the valine pathway at the α -ketoisovalerate intermediate and undergoes four further enzymatic transformations (Fig. 1; Holmberg and Petersen, 1988; Kohlhaw, 2003). By contrast, the pathways of branched-chain amino acid degradation (Fig. 2) are relatively poorly understood. They have, however, been clearly demonstrated to be important for peptide elongation, glutamate recycling, branched-chain

ester formation, and branched-chain fatty acid synthesis (Kandra *et al.*, 1990; Walters and Steffens, 1990; Kroumova *et al.*, 1994; Daschner *et al.*, 1999; Li *et al.*, 2003; Beck *et al.*, 2004; Gu *et al.*, 2010). In addition, during senescence, when carbohydrate availability is limited, the branched-chain amino acids represent a highly important respiratory substrate. Not only do they provide substrates to replenish the tricarboxylic acid (TCA) cycle (Taylor *et al.*, 2004; Engquist *et al.*, 2008), but it has also recently been demonstrated, via interaction with the electron transfer flavoprotein complex, that they provide electrons directly to the mitochondrial electron transport chain (Ishizaki *et al.*, 2005, 2006; Araujo *et al.*, 2010). Moreover, the enzymes [branched-chain amino transferases (BCATs)], which catalyse the interconversion of branched-chain amino acids and branched-chain keto acids have been

comprehensively biochemically characterized in *Arabidopsis* and tomato (Diebold *et al.*, 2002; Schuster and Binder, 2005; Knill *et al.*, 2008; Maloney *et al.*, 2010; Schuster *et al.*, 2010). Mutant and transgenic approaches have also been used to evaluate the functional importance of various BCAT isoforms in *Arabidopsis*, tomato, melon, and *Nicotiana benthamiana* (Knill *et al.*, 2008; Gao *et al.*, 2009; Chen *et al.*, 2010; Gonda *et al.*, 2010; Maloney *et al.*, 2010; Schuster *et al.*, 2010). These genetic analyses have variously highlighted the (species-specific) importance of members of the BCAT gene family in amino acid, glucosinolate, hormone, and volatile organic compound metabolism (Knill *et al.*, 2008; Gao *et al.*, 2009). In previous studies of

Solanum pennellii introgression lines, several robust quantitative trait loci (QTL) were identified for Leu, Ile, and Val accumulation (Schauer *et al.*, 2006, 2008) and the BCAT gene family was evaluated as candidates underlying some of these QTL (Maloney *et al.*, 2010). Our analysis has been extended here to coarse-map the chromosomal locations of an additional 24 genes encoding 23 enzymes associated with the synthesis or degradation of branched-chain amino acids, finding that a further seven of these pathway-associated genes co-located with the above-mentioned QTL, whilst one more, the ketol-acid reductoisomerase (KARI), also mapped close to a co-ordinate QTL. The level of expression of ketol-acid reductoisomerase and dihydroxy-acid dehydratase were found to be invariant in the respective introgression lines with which they co-locate, whereas that of isopropylmalate dehydratase small subunit (hereafter referred to as IPMD) was differentially expressed in introgression lines harbouring the *S. pennellii* allele. Using reverse genetics it was possible to rule out that ketol-acid reductoisomerase and dihydroxy-acid dehydratase (DHAD) played a role in determining fruit BCAA levels, and to confirm that differences in expression of small subunit isopropylmalate dehydratase were, at least partially, responsible for the BCAA QTL co-locating with it on chromosome 6. Despite the lack of effect on fruit BCAA levels in the KARI and DHAD transgenics, the levels of these metabolites in the leaves of all transgenics were dramatically reduced, implying that all three enzymes share in the control of BCAA synthesis in the illuminated leaf. The combined data are discussed here in terms of current models for both the metabolic and the genetic regulation of these essential amino acids.

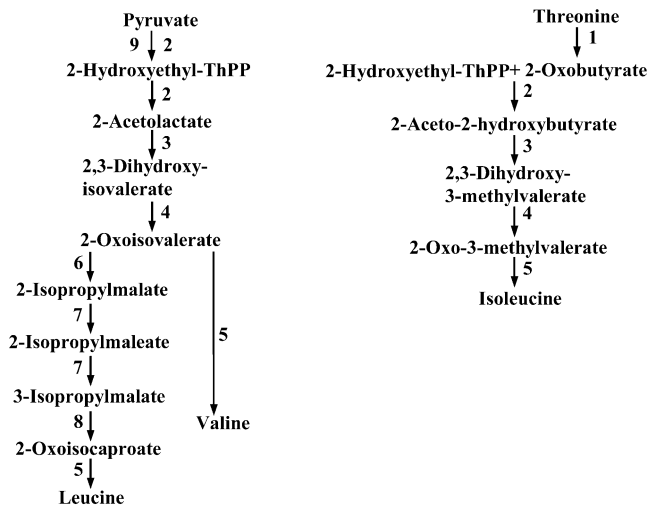


Fig. 1. Biosynthetic pathways of valine, leucine and isoleucine in plants: (1) threonine dehydratase (TD), (2) acetolactate synthase (ALS), (3) ketol-acid reductoisomerase (KARI), (4) dihydroxy-acid dehydratase (DHAD), (5) branched-chain aminotransferase (BCAT), (6) 2-isopropylmalate synthase (IPMS), (7) 3-isopropylmalate dehydratase (IPMD), (8) 3-isopropylmalate dehydrogenase (IPMDH), (9) pyruvate dehydrogenase (PDH).

Materials and methods

Plant material and growth conditions

The *S. pennellii* introgression lines in which each line contains a single introgression from *S. pennellii* (LA 716) in the genetic

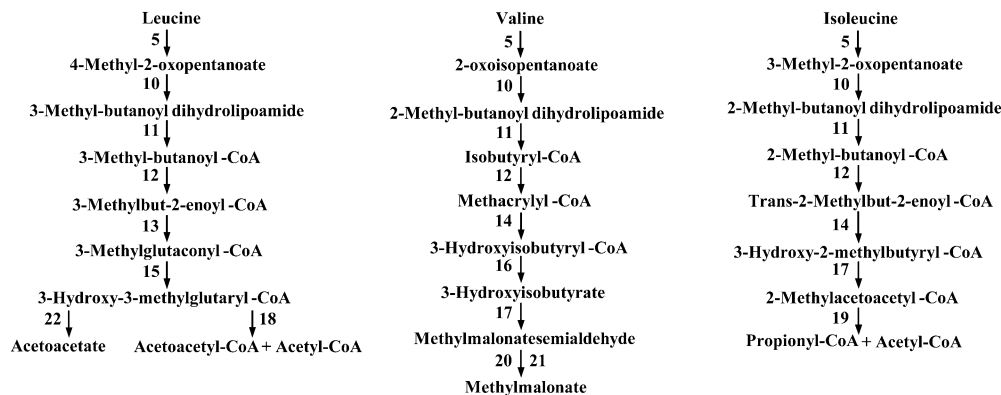


Fig. 2. Catabolic pathways of valine, leucine, and isoleucine in plants. (5) Branched-chain-amino-acid transaminase (BCAT), (10) 3-methyl-2-oxobutanoate dehydrogenase (MOBDH), (11) acyltransferase transferring groups other than amino-acyl groups (ACT), (12) acyl-CoA dehydrogenase (ACAD), (13) methylcrotonyl-CoA carboxylase (MCBB), (14) enoyl-CoA hydratase (ECH), (15) 3-methylglutaconyl-CoA hydratase, (16) 3-hydroxyisobutyryl-CoA hydrolase (HIBCH), (17) 3-hydroxyacyl-CoA dehydrogenase (HACDH), (18) hydroxymethylglutaryl-CoA synthase (HMGS), (19) 3-ketoacyl-CoA thiolase (KAT), (20) aldehyde oxidase AO, (21) aldehyde dehydrogenase (ALDH), (22) hydroxymethylglutaryl-CoA lyase (HMGCL).

background of the processing tomato variety *S. lycopersicum* M82 (Eshed and Zamir, 1995; Pan *et al.*, 2000) were used. Transgenics were created expressing ketol-acid reductoisomerase, dihydroxy-acid dehydratase, and isopropylmalate dehydratase in the antisense orientation in the *S. lycopersicum* Moneymaker background. Plants were grown under long-day conditions (16/8 h day/night cycle) at 22 °C and 50% humidity as described previously in the literature (Carrari *et al.*, 2003).

Southern blot hybridization

Genomic DNA was isolated from leaves using the standard CTAB method (Doyle and Doyle, 1990). 10 µg of DNA were digested with different restriction endonucleases, separated in 0.7% TAE agarose gels and alkali blotted onto Porablot NY Amp nylon membranes (Macherey-Nagel, Germany). Hybridization was performed with P-labelled cDNA clones overnight at 65 °C. The tomato cDNA clones related to BCAA metabolism were obtained from the TIGR Tomato EST database or generated by RT-PCR. They were verified by sequencing and right annotated clones were used as a probes. Clones were mapped by restriction fragment length polymorphism (RFLP) after screening for polymorphism between the parental lines (M82 and *S. pennellii*).

cDNA synthesis and RT-PCR analysis

Total RNA was extracted from the different tissues of tomato according to the method described by Robaglia *et al.* (1993). Oligo(dT)-primed cDNA was synthesized using SuperScript III Reverse Transcriptase (Invitrogen, Germany) and total RNA as the template. After RNase H treatment, 1/10 of the cDNA reaction volume was used for PCR with gene-specific primers (see Supplementary Table S1 at *JXB* online). Expression levels of the KARI, DHAD, and IPMD genes were determined by RT-PCR in leaves of distinct ILs and across different organs and fruit development of cultivated tomato by quantitative RT-PCR. Reactions (10 µl) containing 500 nM gene-specific primers in 1× Power SYBR Green PCR Master Mix (Applied Biosystems, Foster City, CA, USA) plus dilutions of tomato cDNA were run on an ABI7000 Real-Time PCR System (Applied Biosystems, Foster City, CA, USA). Amplification conditions were 2 min at 50 °C, 10 min at 95 °C, 40 cycles each of 15 s at 95 °C followed by 1 min at 60 °C; 15 s at 95 °C; 20 s at 60 °C; and 15 s at 95 °C. Data analysis was performed with the SDS 2.2.1 software (Applied Biosystems). mRNA expression was analysed by Student's *t* test and one-way ANOVA, followed by the Tukey post-hoc test. $P < 0.05$ was considered statistically significant. The amount of KARI, DHAD, and IPMD transcripts in transgenic plants was determined by RT-PCR analysis. Amplification reactions were carried out in a PTC-200 Peltier Thermal Cycler (MJ Research) using the following amplification profile: initial denaturation at 94 °C for 3 min followed by 30 cycles of 94 °C for 30 s, 56 °C for 30 s, and 72 °C for 1 min. Primer sequences can be found in Supplementary Table S1 at *JXB* online. Amplification products were electrophoresed on a 1.2% agarose gel, stained with ethidium bromide, and band intensities were quantified using a Gel Doc XR system (Bio-Rad Laboratories, Germany).

Construction of transgenic plants

The 1327 bp fragment of KARI, the 1897 bp fragment of DHAD, and the 875 bp fragment of IPMD were amplified from tomato cDNA using the gene-specific primers listed in Supplementary Table S1 at *JXB* online. Amplified fragments were cloned first in the pENTR SD/D TOPO vector (Invitrogen) and then sub-cloned into the binary Gateway vector pK2WG7 (Karimi *et al.*, 2002) in the antisense orientation under the control of the 35S promoter, using the Gateway Technology system (Invitrogen). Constructs were introduced into tomato plants (cv. Moneymaker) by an *Agrobacterium*-mediated leaf disc transformation method

(McCormick *et al.*, 1986). Transgenic plants were selected on kanamycin-containing medium (50 mg ml⁻¹).

Extraction and analysis of branched-chain amino acids by GC-MS

Samples of fully developed young leaves and red ripe pericarp fruits at 40 days post-anthesis (dpa) were prepared for metabolite analysis as described previously by Schauer *et al.* (2005a). The level of all metabolites was quantified by gas chromatography-mass spectrometry exactly following the protocol described by Liseč *et al.* (2006), with the exception that the peak identification was optimized to tomato tissues (Roessner-Tunali *et al.*, 2003; Schauer *et al.*, 2005b).

Statistical analysis

Student's *t* tests were performed using the algorithm embedded into Microsoft Excel (Microsoft, Seattle). The term significant is used in the text only when the change in question has been confirmed to be significant ($P < 0.05$) with the *t* test.

Results

Genetic analysis of branched-chain amino acid metabolism in tomato

QTL for the branched-chain amino acids Val, Ile, and Leu have previously been identified in tomato fruit pericarp of introgression lines resulting from the inter-specific cross of *S. lycopersicum* and its wild relative *S. pennellii* (Schauer *et al.*, 2006, 2008). Given the large relatively early estimated evolutionary divergence of these two species (Bermúdez *et al.*, 2008; Kamenetzky *et al.*, 2010), it seems reasonable to anticipate a fair degree of genetic polymorphism between them. Our previous study using this material to characterize the branched-chain amino transferase family revealed that this is indeed the case (Maloney *et al.*, 2010). The choice was made here to map all the other genes associated with branched-chain amino acid biosynthesis and catabolism whose sequences were available from publicly accessible tomato expressed sequence tag (EST) collections (Van der Hoeven *et al.*, 2003) to chromosomal segments as described by Eshed and Zamir (1995). In order to achieve this goal, the EST collection was first searched for sequences corresponding to the 24 enzymes known to be associated with branched-chain amino acid biosynthesis or degradation (Figs 1, 2). The respective ESTs were subsequently cloned from *S. lycopersicum*, genomic DNA of the ILs and parental species was digested with a suite of more than 20 restriction enzymes, and chromosomal map locations of the genes were evaluated. On completion of these analyses, genes encoding 24 independent enzymes could be mapped. Of the 30 genes mapped, including six previously mapped BCAT genes, none mapped to chromosome 4, whereas chromosomes 1, 6, 7, 8, 9, and 11 all harboured three genes and chromosome 12 even harboured four genes associated with branched-chain amino acid metabolism (Fig. 3). When the chromosome positioning of these genes was compared with the previously determined QTL for the branched-chain amino acids, several co-locations were apparent. There are a total of 13 Ile, 17 Leu, and 18 Val QTL with seven of

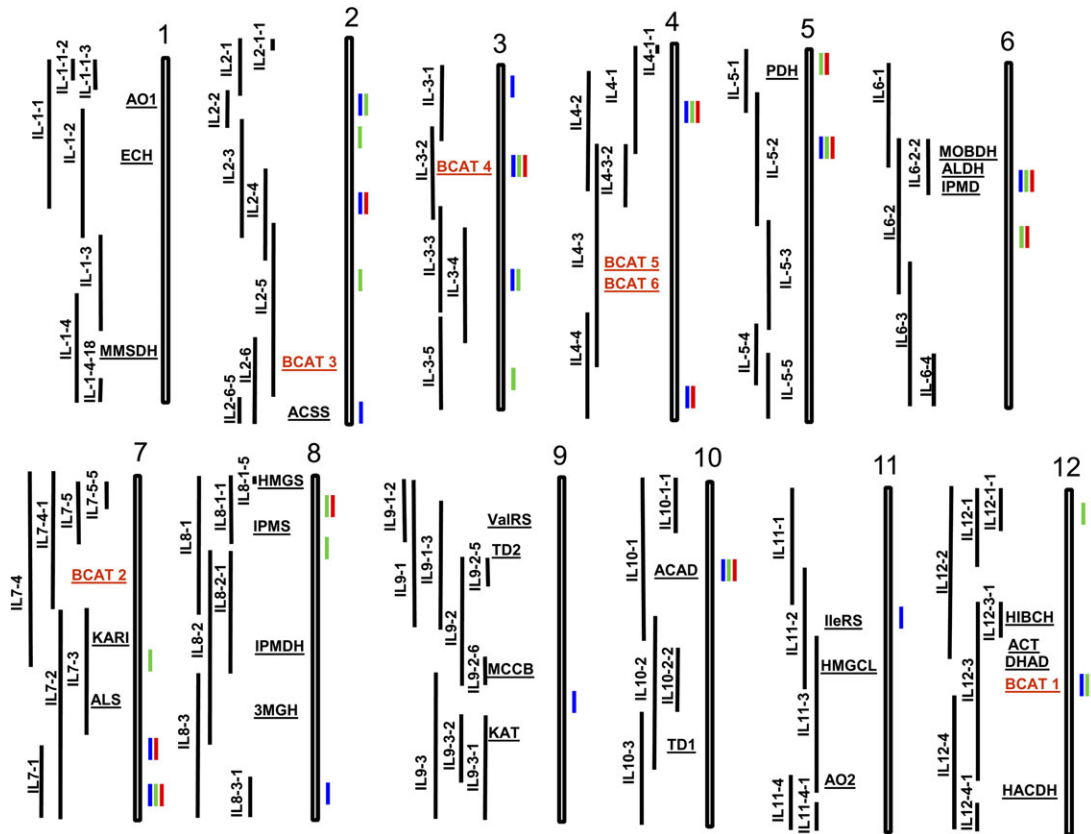


Fig. 3. Map position of the genes involved in metabolism of BCAA and QTLs. The introgressed fragments in ILs are shown on the left of the chromosomes. QTL are indicated to the right of the chromosomes: blue, leucine; red, isoleucine; green, valine. Abbreviations are the same as for Figs 1 and 2 plus MMSDH, methylmalonate semialdehyde dehydrogenase; ValRS, valine tRNA synthase; and IleRS, isoleucine tRNA synthase.

these being common for all three branched-chain amino acids (Fig. 3). Two of the seven major co-ordinate QTL for branched-chain amino acid content (i.e. those in which the change in amino acid content was consistent for Ile, Leu, and Val) were previously documented to co-localize with distinct isoforms of BCAT (Maloney *et al.*, 2010). Whilst our previous study revealed that BCAT1 could well contribute to the QTL, the fact that it also co-localizes with DHAD (TC154979), HIBCH (TC163476), and ACT (TC171921) means that it cannot be ruled out that the QTL is additionally influenced by one of these genes. A further three of these QTL co-localized with the location of structural enzymes in this pathway (IL5-1 with PDH, TC162427; IL6-2-2 with MOBBDH, TC171279, ALDH, TC179074, and IPMD, TC191775; and IL10-1 with ACAD, TC154996). However, two of the co-ordinate QTL did not co-locate with any mapped enzymes (ILs 4-1 and 7-1), although the genes for KARI (TC162067) and ALS (TC154185) mapped close to this QTL. These clusters are particularly interesting in light of the recent identification of several regulons defining secondary metabolism (Osborn *et al.*, 2010). However, it is important to note that, here, the co-clustering genes often belong to both synthetic and degradative pathways of BCAA metabolism, rendering it unlikely that there is a functional significance underlying this pattern.

Following completion of this work a draft tomato genome became available (<http://solgenomics.net/>) and so a search was made for further gene copies of all of the genes described above. In so doing, only a single additional candidate gene, a second DHAD gene sitting at the bottom of chromosome 5 between markers TG351 and TG60, was found. This gene is highly homologous to the one described above so it is somewhat surprising that it was not found in our own mapping study.

Expression analysis in different tomato tissues

Having now fully described the genetic architecture of branched-chain amino acid metabolism, the decision was taken to test the candidature of some of the co-localizing genes. For this purpose, IPMD, DHAD, and KARI were selected on the basis of the (near) co-localization and the positioning of these enzymes within the BCAA biosynthetic pathways. To gain a better understanding of the different roles of each enzyme, expression analysis was performed by quantitative reverse transcription (qRT)-PCR. The tissues tested were shoots, leaves, and flowers as well as fruit harvested 10, 20, 30, and 40 dpa. Expression of KARI was essentially constitutive; however, IPMD and DHAD displayed different levels of expression; IPMD displaying high expression in leaves and fruits harvested at 40 dpa, whereas

DHAD was, by contrast, relatively lowly expressed in these tissues but highly expressed in younger fruit (Fig. 4).

The expression levels of KARI and DHAD in the introgression lines harbouring the respective *S. pennellii* alleles of these genes was invariant from that of the M82 control. Intriguingly, however, the two introgression lines

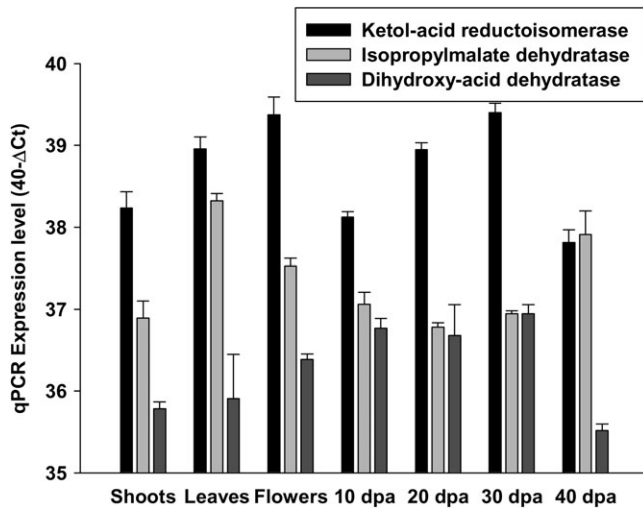


Fig. 4. Expression profile of ketol-acid reductoisomerase (KARI), dihydroxy-acid dehydratase (DHAD), and 3-isopropylmalate dehydratase (IPMD) genes in different tissues of tomato. Transcript levels were determined by real-time PCR. Data represent mean values \pm SE from three independent biological replicates. dpa, Days post-anthesis.

IL6-2 and IL6-2-2, both possessing the *S. pennellii* allele of IPMD, demonstrate substantial differences in the amount of IPMD transcript (Fig. 5C). IL6-2 differs from IL6-2-2 by the presence of a longer *S. pennellii* genomic region upstream of the 5' end of the IPMD gene (corresponding to the distance between markers TG177 and TG279). Since we did not map any structural gene encoding either biosynthetic or catabolic enzyme in this region, it would seem reasonable to assume that the observed differences may be determined by a regulatory gene. Indeed, a detailed analysis of the genomic scaffolds of the draft tomato genome encompassing this region (<http://solgenomics.net/>) revealed a total of 17 transcription factors (TFs) and transcription-like proteins in this region in close proximity to the 5' end of IPMD (see Supplementary Table S2 at *JXB* online), however, it is too early to say whether any of these are indeed responsible for the observed changes.

Reverse genetic analysis of KARI, IPMD, and DHAD

In order to test the importance of the above-discussed candidate genes directly, a transgenic approach was adopted, wherein the expression levels of KARI, IPMD, and DHAD were individually reduced by using the antisense approach. For this purpose, segments of all three genes were cloned in an antisense orientation in the vector pK2WG7 under the control of the constitutive CaMV 35S promoter. Transformants were selected primarily on the basis of antibiotic resistance followed by subsequent screening by RT-PCR. The relative expression levels in leaf samples of the selected lines are presented in Fig. 6, which shows that substantial

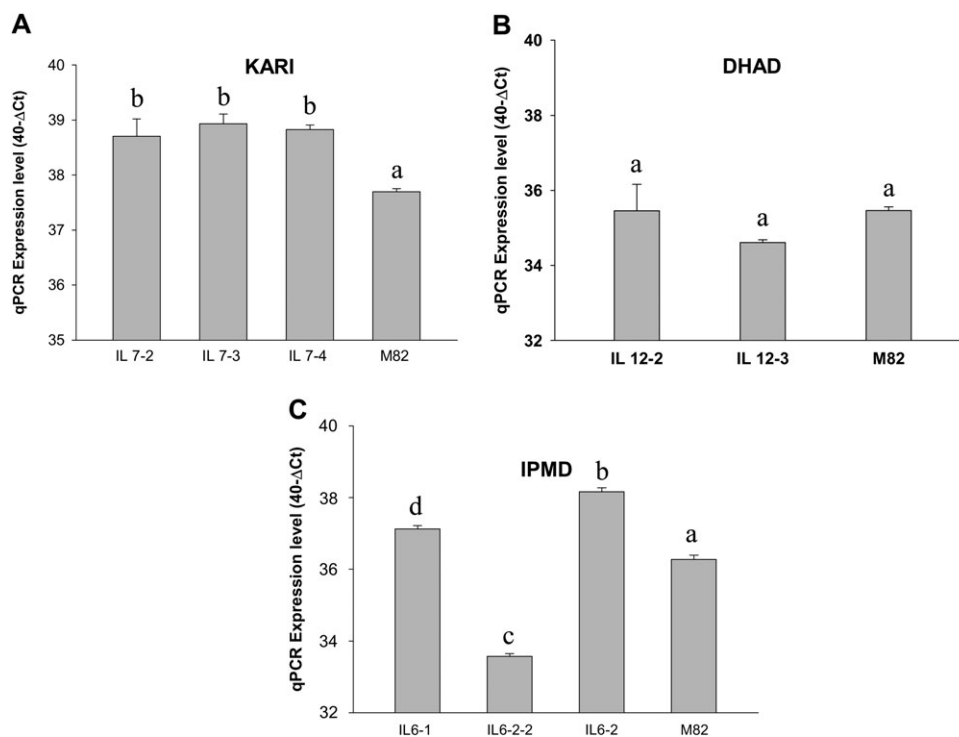


Fig. 5. Expression of Ketol-acid reductoisomerase (KARI), dihydroxy-acid dehydratase (DHAD), and small subunit 3-isopropylmalate dehydratase (IPMD) analysed by real-time quantitative RT-PCR in *Solanum lycopersicum* (cv. M82) and distinct introgression lines (ILs). Data represent mean values \pm SE from three independent biological replicates with two technical replicates for each.

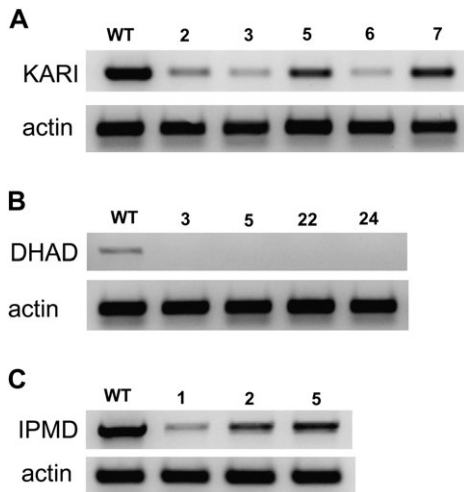


Fig. 6. Expression analysis of antisense suppression lines of tomato. (A) Transcript levels of ketol-acid reductoisomerase (KARI), (B) dihydroxy-acid dehydratase (DHAD), and (C) 3-isopropylmalate dehydratase (IPMD) in transgenic plants carrying corresponding antisense construct and control untransformed plants analysed by RT-PCR.

reductions in expression were seen for five KARI lines (numbers 2, 3, 6, and 7), four DHAD lines (numbers 3, 5, 22, and 24 which were all reduced to below detection levels), and two IPMD lines (numbers 1 and 2).

The levels of BCAAs in samples harvested from source leaves of 8-week-old plants were evaluated next using an established GC-MS protocol (Fernie *et al.*, 2004). In each set, the transgenic down-regulated lines essentially displayed reduced levels of all three metabolites (Fig. 7). For example, in DHAD antisense plants the contents of BCAA were reduced by 24–56% (see Supplementary Table S4 at *JXB* online). At the same time it should be noted that reduction level of BCAA contents strongly correlated with the level of transcript down-regulation. In the most extreme cases a milder reduction of transcript had no effect on BCAA level. KARI transgenic plants (line 7) which retained the expression of the gene at a level of about 70% of the wild-type expression did not show any reduction in the content of BCAA (see Supplementary Table S3 at *JXB* online), whereas in the leaves of the strongest transgenic lines 3 and 6, in which the KARI transcript level was reduced to 27% of the wild-type level, the content of BCAA reached only 49–79% of that in the control plants. Antisense expression of the IPMD gene resulted in a significant decrease in BCAA content (2-fold) only when the level of IPMD expression in transgenic plants was decreased to below 30% of the wild-type level. Given that the QTL had previously been detected in red-ripe fruit, the BCAA content was next determined in such samples harvested from the transgenics. The KARI lines were essentially unaltered with only one statistically significant change in content in any of the lines (Fig. 8A). DHAD showed a highly variable content, however, this appears to be unrelated to the altered expression level, since the BCAA content increases in lines 22 and 24 yet decreases in line 5 and is unaltered in line 3

(Fig. 8B). By contrast, IPMD revealed co-ordinately elevated levels of all three BCAAs in the lines, exhibiting the greatest reduction in gene expression (Fig. 8C), suggesting that it is indeed responsible for changes in their content. In order to characterize this better, the localization of the gene was studied with respect to the levels of the BCAAs in both the overlapping lines IL6-2 and IL62-2 (see map position on the chromosome and the Southern blot hybridized with *S. lycopersicum* IMPD). Perhaps surprisingly in light of the fact that the IPMD gene lies in the overlapping region but the lines exhibit differential expression of the gene, was the observation that the greatest change in BCAA levels was observed in the line with invariant expression (Fig. 9). This suggests that the QTL is not merely a simple expression QTL but a mixed QTL which exhibits altered expression and protein quality.

Having initially focused on the BCAA levels of all three transgenics, our studies were broadened to evaluate the levels of other metabolites which could not be detected within our chromatograms. Starting with the leaf material, quite extensive changes were observed in the metabolite profiles of the KARI antisense lines. Whilst many of these changes were minor or inconsistent across lines, several of them were notable. For example, three of the four lines exhibited increases in the level of serine, cysteine, and phenylalanine, whilst all four lines displayed elevated sucrose levels, and at least three of the lines displayed decreased levels of dehydroascorbate and quinate (see Supplementary Table S3 at *JXB* online). A similar picture was observed when other metabolic consequences of down-regulating DHAD in leaves was evaluated, with all four transgenic lines displaying clear decreases in their content of cysteine, lysine, and glycine, whilst fructose and sucrose increased in all four lines, and putrescine decreased in three of them (see Supplementary Table S4 at *JXB* online). In addition, the levels of succinate were decreased, whilst citrate and particularly glutarate increased massively in all DHAD lines. When leaf material of the IPMD lines was evaluated, many changes were observed, however, those which are consistent are once again a decrease in cysteine, phenylalanine, dehydroascorbate, and putrescine whilst, by contrast, fructose, sucrose, and citrate increased (see Supplementary Table S5 at *JXB* online).

A similar evaluation of the chromatograms determined for the red-ripe fruit of the transgenics was performed next, starting with the KARI antisense lines. It was perhaps surprising to see that they exhibited very few conserved changes across the lines. However, arginine levels were increased in three of the four lines, as was maltose and dehydroascorbate, whilst inositol was increased in all four of the transgenics (see Supplementary Table S6 at *JXB* online). Even fewer conserved changes were seen in the ripe fruits of the DHAD lines; whilst there were a considerable number of changes, many of them were in opposing directions in the different lines but threonine, inositol, and glycerol were all increased in three of the four transgenic lines (see Supplementary Table S7 at *JXB* online). The IPMD lines, however, displayed clearer changes, although

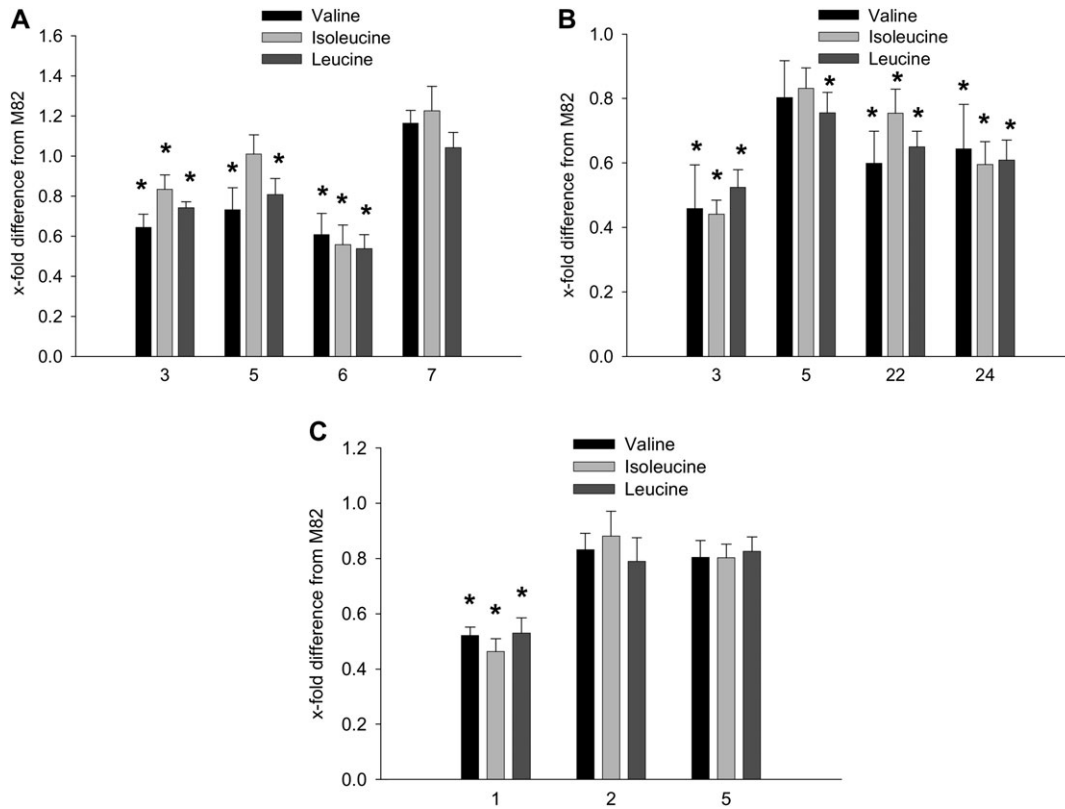


Fig. 7. GC-MS analysis of BCAA content in the leaves of transgenics. (A, B, C) Data of the evaluation of plants expressing antisense constructs for Ketol-acid reductoisomerase (KARI), dihydroxy-acid dehydratase (DHAD), and 3-isopropylmalate dehydratase (IPMD), respectively. Data represent means \pm SE from six independent biological replicates. Asterisks show statistically significant changes according to Student's *t* test ($P < 0.05$).

they were largely confined to the two lines exhibiting the strongest degree of inhibition of expression. These lines showed similar patterns of change in the levels of phenylalanine, arginine, tyrosine, and histidine, as well as dehydroascorbate, phosphoric acid, inositol, and sucrose, and massive changes in the levels of maltose. In all cases the levels of these metabolites were found at increased levels with respect to the wild type (see Supplementary Table S8 at *JXB* online).

Discussion

BCAAs are of crucial importance in tomato fruit not only as essential amino acids for food and feed (Schulze-Siebert *et al.*, 1984; Hagelstein *et al.*, 1997), but they also potentially contribute greatly to flavour as the precursors of volatiles (Gonda *et al.*, 2010). Previous studies have described the determination of QTL for BCAAs in tomato fruit (Schauer *et al.*, 2008, 2006), and shown that two of these are probably controlled by the branched-chain amino transferases BCAT1 and 4 (Maloney *et al.*, 2010). The mapping of candidate structural genes has been extended here to the entire pathways of BCAA synthesis and degradation and the reverse genetic characterization of KARI, DHAD, and IPMD is described. In all instances, antisense transgenic lines were created, as well as characterizing the expression levels of each gene in both the wild type

across development and in the transgenics and introgression lines of interest. In addition, cloning and sequencing of the alleles of all three genes was carried out (amino acid sequence alignments are provided in Supplementary Figs S1–S3 at *JXB* online). The ultimate aim of these experiments was to understand the metabolic and genetic regulation of branched-chain amino acid metabolism in plants better.

This mapping approach allowed a total of 24 novel localizations of genes encoding enzymes of BCAA metabolism to be identified, whilst subsequent perusal of the draft genome sequence allowed a 25th locus to be identified. Of the seven QTL affected in all three BCAAs, a further seven of these pathway-associated genes co-located with the above-mentioned QTL were identified, whilst one more KARI additionally mapped relatively close to a co-ordinate QTL and was co-expressed in ILs which had one to two BCAA QTL. Therefore two co-ordinate QTL were left for which absolutely no overlap could be identified—those in IL4-1 and IL5-2. Whilst this may appear surprising, it is not without precedent since similar findings have been reported in studies on tomato pigment metabolism (Liu *et al.*, 2003) and in flavone metabolism in maize silks (McMullen *et al.*, 1998). It was hypothesized that the co-location of the IPMD with the IL6-2 QTL and the DHAD with the IL12-3 QTL were attractive candidate genes despite the overlap of the latter with the previously characterized BCAT1 (Maloney *et al.*, 2010). In

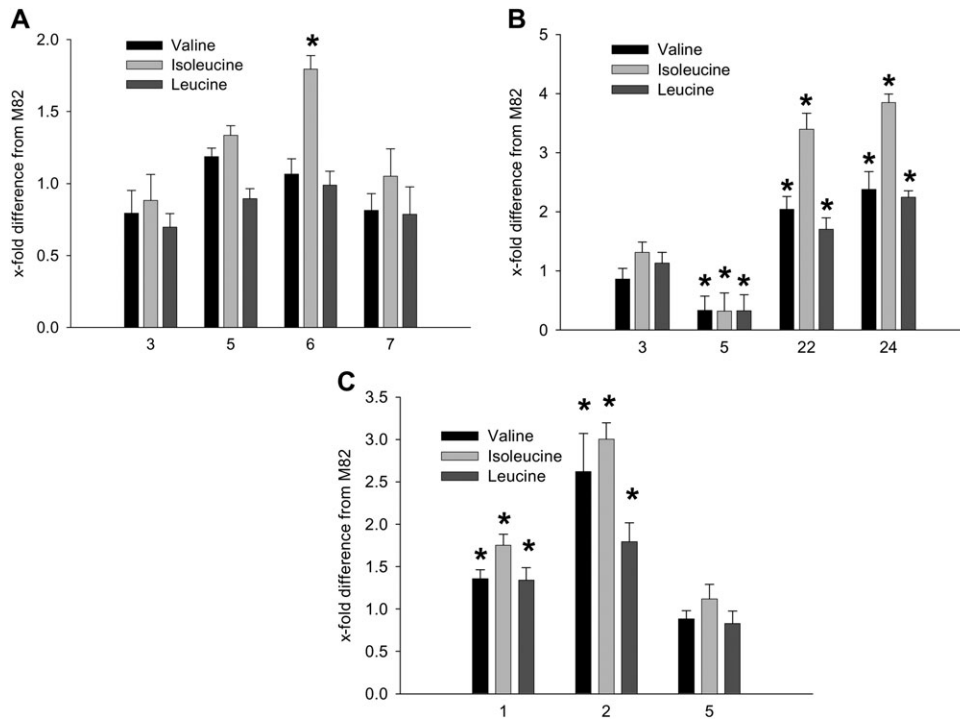


Fig. 8. GC-MS analysis of BCAA content in the red ripe fruits of transgenics. (A, B, C) Data of the evaluation of plants expressing antisense constructs for ketol-acid reductoisomerase (KARI), dihydroxy-acid dehydratase (DHAD), and 3-isopropylmalate dehydratase (IPMD), respectively. Data represent means \pm SE from six independent biological replicates. Asterisks show statistically significant changes according to Student's *t* test ($P < 0.05$).

addition, the choice was made to characterize KARI, despite the fact that it did not exactly co-localize, given its structural location in the biosynthetic pathway and agronomical importance as a herbicide target (Fig. 1; Leung and Guddat, 2009).

The expression pattern of the three genes chosen to be targeted was quite distinct, with only DHAD expression reflecting the levels of BCAAs in the various tissues and across fruit development (Carrari *et al.*, 2006; Do *et al.*, 2010; Maloney *et al.*, 2010), whereas KARI fluctuated throughout fruit development and IPMD expression troughed at 20 dpa before gradually recovering (Fig. 4). When compared with BCAT1 and BCAT4, which had previously been characterized, DHAD displayed a similar pattern of expression to BCAT4, which was also demonstrated to operate largely in the synthetic direction (Maloney *et al.*, 2010), whilst the others did not show a similar expression pattern to either. Despite the seemingly good correlation between DHAD expression and BCAA content, it was not possible to obtain convincing evidence that it contributes to the BCAA QTL harboured by IL 12-3-1, because whilst two of the transgenic lines displayed elevated levels of the BCAAs, one displayed reduced levels of these metabolites. BCAT1 also mapped to this IL, but our previous claims that polymorphism in BCAT1 is responsible for the quantitative trait variation at this genetic locus (Maloney *et al.*, 2010), are in no way negated by the more detailed studied of the genetic architecture of BCAA metabolism presented here. Not only do the DHAD transgenics show no consistent alteration in BCAA levels in fruit (Fig. 8), but nor do the introgression lines spanning this

region display a change in the expression level of the gene (Fig. 6), suggesting that the three amino acid polymorphisms between the *S. lycopersicum* and *S. pennellii* alleles (see Supplementary Fig. S2 at *JXB* online) do not alter the properties of this enzyme in a manner critical enough to impact the BCAA content of the fruit. This conclusion is perhaps somewhat lessened by the fact that, following the analyses of these transgenic lines, a second DHAD locus was identified in the tomato genome. However, whilst possible compensatory effects of this gene may explain the lack of effects in the transgenics, the close homology of the genes would make it more likely that the expression of both genes was reduced in the transformants. These observations provide additional support to our previous claim, that the polymorphism in BCAT1 is responsible for the quantitative trait variation at this genetic locus (Maloney *et al.*, 2010). Furthermore, it should be noted that the fact that microbial BCAA biosynthesis appears to be largely transcriptionally regulated (Holakto *et al.*, 2009) and that DHAD is a key point for such regulation does, however, suggest that this enzyme may have other key roles in plants.

The candidature of KARI could also effectively be ruled out as a causal gene for fruit BCAA content, since antisense plant lines exhibiting reduced expression of the corresponding mRNA revealed no changes in BCAA content, with the exception of an increase in isoleucine content in line 6 (Fig. 8). Moreover, the expression of KARI in the introgression lines expressing the *S. pennellii* allele was essentially unaltered from the of the M82 control (Fig. 6). Sequencing of the alleles again revealed polymorphism (this time in four

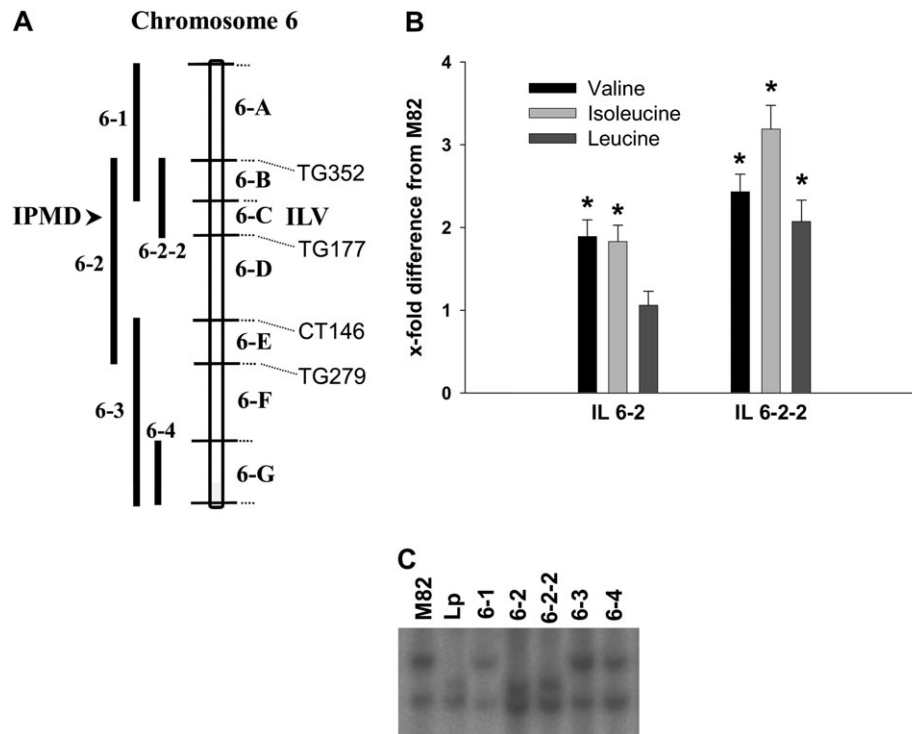


Fig. 9. Mapping of the gene encoding small subunit of IPMD and branched-chain QTL. (A) Map positions of IPMD and BCAA QTLs. I, isoleucine; L, leucine; V, valine. (B) Content of BCAAs in red tomato fruits (40 dpa) measured by GC-MS. Data represent means \pm SE from six independent biological replicates. Asterisks show significance according to Student's *t* test ($P < 0.05$). (C) Southern-blot analysis of ILs.

residues; see Supplementary Fig. S1 at *JXB* online). However, this is not entirely surprising when the predicted level of polymorphism between *S. lycopersicum* and *S. pennellii* is considered (Nesbitt and Tanksley, 2002; Kamenetsky *et al.*, 2010). More critically, they are also outside of the essential Mg^{2+} binding points, polar contacts with NADPH, dimer loops, and the C-terminal tail that have been determined by comparison of the crystal structure of plant and non-plant enzymes alike (Leung and Guddat, 2009). That KARI does not appear to have a great influence on the level of fruit BCAA is, in itself, perhaps not overly surprising, given the fact that it did not in fact co-localize to a co-ordinate QTL, however, the fact that it is a herbicidal target (Durner *et al.*, 1993), would suggest that there may be plenty of value in further characterizing the lines generated here.

By contrast with the above two examples, our studies supported an underlying role for IPMD in determining the fruit BCAA content with antisense lines displaying a strong increase in this parameter, at least once expression is reduced below a certain threshold. Moreover, the IPMD gene co-localizes to both IL6-2 and IL6-2-2, with the level of expression being moderately increased in the former but decreased in the latter (Fig. 6). Whilst a number of TFs have been identified that may be responsible for the differences in these lines, another, perhaps more likely explanation, is that the *S. pennellii* allele is less efficient than the *S. lycopersicum* one. Such differences in protein quality have already been demonstrated following the approach

described here both for the cell wall invertase LIN5 (Fridman *et al.*, 2004; Zanon *et al.*, 2009) and BCAT4 (Maloney *et al.*, 2010). That said, expression levels appear to be the mechanism responsible for the QTL for BCAA determined by BCAT1 at IL12-3 (Maloney *et al.*, 2010) and it cannot be formally ruled out that the situation observed here is the effect of combined transcriptional and post-translational mechanisms. Evaluation of the sequence of both alleles does not give strong hints to what would cause this effect, since it is not easy to discern if the only non-conserved sequence polymorphism (L to P) corresponds with any of the critical residues of the determined crystal structure of *Thermus thermophilus* (Nango *et al.*, 2009).

Looking beyond our immediate aims in this study, some further interesting observations were made, namely that, despite the mixed response on fruits, all three sets of transgenics displayed a similar tendency of decreased BCAAs in the source leaves (Fig. 7). This observation is consistent with the enhanced importance of the enzymes in this tissue which must generate these metabolites *de novo*, since in contrast to the situation in the fruit (Valle *et al.* 1998; Do *et al.*, 2010) none will be delivered from other tissues. Once further transgenic lines in the pathway have been created, it will be interesting to perform a pathway-wide analysis of the metabolic control resident in this pathway in an analogous manner to that carried out for the sucrose to starch conversion in potato (Geigenberger *et al.*, 2004). Other interesting leads for future research are the

changes in other metabolites, especially certain sugars, organic acids, and amino acids which occur in some, or all, of the transgenic sets, in either the leaf or fruit. It is interesting that these changes are sometimes greater than those in the BCAAs themselves and as such support the growing body of evidence concerning the high functional connectivity within pathways of amino acid metabolism (Angelovici *et al.*, 2009; Gu *et al.*, 2010) as well as within central metabolism in general (Sulpice *et al.*, 2010). However, considerable further research will be required in order to understand fully both the metabolic and signalling functions which control such interactions.

In summary, an extensive study of BCAA metabolism in tomato fruit has been carried out here, in order to complement our earlier study of the BCAT gene family in tomato (Maloney *et al.*, 2010). These studies revealed that, of the seven co-ordinate QTL, only four harboured candidate structural genes associated with the metabolism of these compounds. It was possible to demonstrate here that IPMD represents an important step in the determination of tomato fruit BCAA levels in addition to BCATs1 and 4 which were characterized in our previous study. That said, evaluation of the BCAA levels in the leaves of all three sets of transgenics studied here revealed that KARI and DHAD, in addition to IPMD, play an important role in determining the levels of these compounds in source leaves. The lack of a clear visible phenotype under normal nutrient-replete conditions suggests that, in order fully to determine the roles of each individual enzyme, it will probably require their growth in response to a wide range of stressors to be tested. The fact that several of the co-ordinate QTL do not co-localize to structural genes suggests that several regulatory genes remain to be identified which control the accumulation of these important metabolites within the tomato fruit.

Supplementary data

Supplementary data can be found at *JXB* online.

Supplementary Table S1. Primer sequences used in the study.

Supplementary Table S2. List of transcription factors which are encoded by the *S. pennellii* alleles in introgression line IL IL6-2 but not IL6-2-2.

Supplementary Table S3. Metabolic profiling of leaves of the KARI antisense lines by GC-MS.

Supplementary Table S4. Metabolic profiling of leaves of the DHAD antisense lines by GC-MS.

Supplementary Table S5. Metabolic profiling of leaves of the IPMD antisense lines by GC-MS.

Supplementary Table S6. Metabolic profiling of red ripe fruit of the KARI antisense lines by GC-MS.

Supplementary Table S7. Metabolic profiling of red ripe fruit of the DHAD antisense lines by GC-MS.

Supplementary Table S8. Metabolic profiling of red ripe fruit of the IPMD antisense lines by GC-MS.

Supplementary Fig. S1. Amino acid sequences comparison of KARI between *S. lycopersicum* and *S. pennellii*.

Supplementary Fig. S2. Amino acid sequences comparison of DHAD between *S. lycopersicum* and *S. pennellii*.

Supplementary Fig. S3. Amino acid sequences comparison of IPMD between *S. lycopersicum* and *S. pennellii*.

Acknowledgements

This work was supported in part by EUSol (grant number FOOD-CT-2006-016214 and in part by the ERAnet project TomQML.

References

- Angelovici R, Fait A, Zhu X, Szymanski J, Feldmesser E, Fernie AR, Galili G.** 2009. Deciphering transcriptional and metabolic networks associated with lysine metabolism during *Arabidopsis* seed development. *Plant Physiology* **151**, 2058–2072.
- Araujo WL, Ishizaki K, Nunes-Nesi A, et al.** 2010. Identification of the 2-hydroxyglutarate and isovaleryl-CoA dehydrogenases as alternative electron donors linking lysine catabolism to the electron transport chain of *Arabidopsis* mitochondria. *The Plant Cell* **22**, 1549–1563.
- Beck HC, Hansen AM, Lauritsen FR.** 2004. Catabolism of leucine to branched-chain fatty acids in *Staphylococcus xylosum*. *Journal of Applied Microbiology* **96**, 1185–1193.
- Bermúdez L, Urias U, Milstein D, Kamenetzky L, Asis R, Fernie AR, Van Sluys MA, Carrari F, Rossi M.** 2008. A candidate gene survey of quantitative trait loci affecting chemical composition in tomato fruit. *Journal of Experimental Botany* **59**, 2875–2890.
- Carrari F, Nunes-Nesi A, Gibon Y, Lytovchenko A, Loureriro ME, Fernie AR.** 2003. Reduced expression of aconitase results in an enhanced rate of photosynthesis and marked shifts in carbon partitioning in illuminated leaves of wild species tomato. *Plant Physiology* **133**, 1322–1335.
- Carrari F, Baxter C, Usadel B, et al.** 2006. Integrated analysis of metabolite and transcript levels reveals the metabolic shifts that underlie tomato fruit development and highlight regulatory aspects of metabolic network behavior. *Plant Physiology* **142**, 1380–1396.
- Chen H, Saksa K, Zhao F, Qiu J, Xiong L.** 2010. Genetic analysis of pathway regulation for enhancing branched-chain amino acid biosynthesis in plants. *The Plant Journal* **4**, 573–583.
- Daschner K, Thalheim C, Guha C, Brennicke A, Binder S.** 1999. In plants a putative isovaleryl-CoA-dehydrogenase is located in mitochondria. *Plant Molecular Biology* **39**, 1275–1282.
- Durner J, Knörzer OC, Böger P.** 1993. Ketol-acid reductoisomerase from barley (*Hordeum vulgare*): purification, properties and specific inhibition. *Plant Physiology* **103**, 903–910.
- de Kraker JW, Luck K, Textor S, Tokuhisa JG, Gershenzon J.** 2007. Two *Arabidopsis* genes (IPMS1 and IPMS2) encode isopropylmalate synthase, the branchpoint step in the biosynthesis of leucine. *Plant Physiology* **143**, 970–986.
- Diebold R, Schuster J, Däschner K, Binder S.** 2002. The branched-chain amino acid transferase gene family in *Arabidopsis*

- encodes plastid and mitochondrial proteins. *Plant Physiology* **129**, 540–550.
- Do PT, Prudent M, Sulpice R, Causse M, Fernie AR.** 2010. The influence of fruit load on the tomato pericarp metabolome in a *Solanum chmielewskii* introgression line population. *Plant Physiology* **154**, 1128–1142.
- Doyle JJ, Doyle JL.** 1990. Isolation of plant DNA from fresh tissue. *Focus* **12**, 13–15.
- Engqvist M, Drincovich MF, Flugge UI, Maurino VG.** 2009. Two D-2-hydroxy-acid dehydrogenases in *Arabidopsis thaliana* with catalytic capacities participate in the last reactions of the methylglyoxal and beta-oxidation pathways. *Journal of Biological Chemistry* **284**, 25026–25037.
- Eshed Y, Zamir D.** 1995. An introgression line population of *Lycopersicon pennellii* in the cultivated tomato enables the identification and fine mapping of yield-associated QTL. *Genetics* **141**, 1147–1162.
- Fernie AR, Krotzky AJ, Trethewey RN, Willmitzer L.** 2004. Innovation- metabolite profiling: from diagnostics to systems biology. *Nature Reviews Molecular Cell Biology* **5**, 763–769.
- Fridman E, Carrari D, Liu YS, Fernie AR, Zamir D.** 2004. Zooming in on a quantitative trait for tomato yield using interspecific introgressions. *Science* **305**, 1786–1789.
- Gao F, Wang C, Wei C, Yi L.** 2009. A branched-chain aminotransferase may regulate hormone levels by affecting KNOX genes in plants. *Planta* **230**, 611–623.
- Geigenberger P, Stitt M, Fernie AR.** 2004. Metabolic control analysis and regulation of the conversion of sucrose to starch in growing potato tubers. *Plant, Cell and Environment* **6**, 655–673.
- Gonda I, Bar E, Portnoy V, Lev S, Burger J, Schaffer AA, Tadmor Y.** 2010. Branched-chain and aromatic amino acid catabolism into aroma volatiles in *Cucumis melo* L. fruit. *Journal of Experimental Botany* **61**, 1111–1123.
- Gu L, Jones D, Last RL.** 2010. Broad connections in the *Arabidopsis* seed metabolic network revealed by metabolite profiling of an amino acid catabolism mutant. *The Plant Journal* **61**, 579–590.
- Hagelstein P, Sieve B, Klein M, Jans H, Schultz G.** 1997. Leucine synthesis in chloroplasts: leucine/isoleucine aminotransferase and valine aminotransferase are different enzymes in spinach chloroplasts. *Journal of Plant Physiology* **150**, 23–30.
- Holatkó J, Elisakova V, Prouza M, Sobotka M, Nesvera J, Patek M.** 2009. Metabolic engineering of the L-valine biosynthesis pathway in *Cornibacterium glutamicum* using promoter activity modulation. *Journal of Biotechnology* **139**, 203–210.
- Holmberg S, Petersen JG.** 1988. Regulation of isoleucine-valine biosynthesis in *Saccharomyces cerevisiae*. *Current Genetics* **13**, 207–217.
- Ishizaki K, Larson TR, Schauer N, Fernie AR, Graham IA, Leaver CJ.** 2005. The critical role of *Arabidopsis* electron-transfer flavoprotein: ubiquinone oxidoreductase during dark-induced starvation. *The Plant Cell* **17**, 1–14.
- Ishizaki K, Schauer N, Larson TR, Graham IA, Fernie AR, Leaver CJ.** 2006. The mitochondrial electron transfer flavoprotein complex is essential for survival of *Arabidopsis* in extended darkness. *The Plant Journal* **47**, 751–760.
- Kamenetzky L, Asís R, Bassi S, et al.** 2010. Genomic analysis of wild tomato (*Solanum pennellii*) introgressions determining metabolic and yield associated traits. *Plant Physiology* **152**, 1772–1786.
- Kandra G, Severson R, Wagner GJ.** 1990. Modified branched-chain amino acid pathways give rise to acyl acids of sucrose esters exuded from tobacco leaf trichomes. *European Journal of Biochemistry* **188**, 385–391.
- Karimi M, Inzé D, Depicker A.** 2002. GATEWAY™ vectors for *Agrobacterium*-mediated plant transformation. *Trends in Plant Science* **7**, 193–195.
- Knill T, Schuster J, Reichelt M, Geershenzon J, Binder S.** 2008. *Arabidopsis* branched-chain aminotransferase 3 functions in both amino acid and glucosinolate biosynthesis. *Plant Physiology* **146**, 1028–1039.
- Kohlhaw GB.** 2003. Leucine biosynthesis in fungi: entering metabolism through the back door. *Microbiology and Molecular Biology Reviews* **67**, 1–6.
- Kroumova AB, Xie Z, Wagner GJ.** 1994. A pathway for the biosynthesis of straight and branched, odd- and even-length, medium-chain fatty acids in plants. *Proceedings of the National Academy of Sciences, USA* **91**, 11437–11441.
- Leung EWW, Guddat LW.** 2009. Conformation changes in a plant ketol-acid reductoisomerase upon Mg²⁺ and NADPH binding as revealed by two crystal structures. *Journal of Molecular Biology* **389**, 167–182.
- Li L, Thipyapong P, Breeden DC, Steffens JC.** 2003. Overexpression of a bacterial branched-chain alpha-keto acid dehydrogenase complex in *Arabidopsis* results in accumulation of branched-chain acyl-CoAs and alteration of free amino acid composition in seeds. *Plant Science* **165**, 1213–1219.
- Liu YS, Gur A, Ronen G, Causse M, Damidaux R, Buret M, Hirschberg J, Zamir D.** 2003. There is more to tomato fruit color than candidate carotenoid genes. *Plant Biotechnology Journal* **1**, 195–207.
- Lisec J, Schauer N, Kopka J, Willmitzer L, Fernie AR.** 2006. Gas chromatography mass spectrometry-based metabolite profiling in plants. *Nature Protocols* **1**, 387–396.
- Maloney GS, Kochevenko A, Tieman DM, Tohge T, Krieger U, Zamir D, Taylor MG, Fernie AR, Klee HJ.** 2010. Characterization of the branched-chain amino acid amino transferase enzyme family in tomato. *Plant Physiology* **153**, 925–936.
- McCormick S, Niedermeyer J, Fry J, Barnason A, Horsch R, Fraley R.** 1986. Leaf disk transformation of cultivated tomato (*Lycopersicon esculentum*) using *Agrobacterium tumefaciens*. *Plant Cell Reports* **5**, 81–84.
- McMullen MD, Byrne PF, Snook ME, Wiseman BR, Lee EA, Widstrom NW, Coe EH.** 1998. Quantitative trait loci and metabolic pathways. *Proceedings of the National Academy of Sciences, USA* **95**, 1996–2000.
- Nango E, Yamamoto T, Kumasaka T, Eguchi T.** 2009. Crystal structure of 3-isopropylmalate dehydrogenase in complex with NAD(+)

and a designed inhibitor. *Bioorganic and Medicinal Chemistry* **22**, 7789–7794.

Nesbitt TC, Tanksley SD. 2002. Comparative sequencing in the genus *Lycopersicon*: implications for the evolution of fruit size in the domestication of cultivated tomatoes. *Genetics* **162**, 365–379.

Osborn A. 2010. Gene clusters for secondary metabolic pathways: an emerging theme in plant biology. *Plant Physiology* **154**, 531–535.

Pan Q, Liu YS, Budai-Hadrian O, Carmel-Goren L, Zamir D, Fluhr R. 2000. Comparative genetics of nucleotide binding site-leucine rich repeat resistance homologues in the genomes of two dicotyledons: tomato and *Arabidopsis*. *Genetics* **155**, 309–322.

Robaglia C, Bruening G, Haseloff J, Gerlach WL. 1993. Evolution and replication of tobacco ringspot virus satellite RNA mutants. *EMBO Journal* **12**, 2969–2976.

Roessner-Tunali U, Hegemann B, Lytovchenko A, Carrari F, Bruedigam C, Granot D, Fernie AR. 2003. Metabolic profiling of transgenic tomato plant overexpressing hexokinase reveals that the influence of hexose phosphorylation diminishes during fruit development. *Plant Physiology* **133**, 84–99.

Schulze-Siebert D, Heineke D, Scharf H, Schultz G. 1984. Pyruvate-derived amino acids in spinach chloroplasts: synthesis and regulation during photosynthetic carbon metabolism. *Plant Physiology* **76**, 465–471.

Schauer N, Zamir D, Fernie AR. 2005a. Metabolic profiling of leaves and fruit of wild species tomato: a survey of the *Solanum lycopersicum* complex. *Journal of Experimental Botany* **56**, 297–307.

Schauer N, Steinhauser D, Strelkov S, et al. 2005b. GC-MS libraries for the rapid identification of metabolites in complex biological samples. *FEBS Letters* **579**, 1332–1337.

Schauer N, Semel Y, Roessner U, et al. 2006. Comprehensive metabolic profiling and phenotyping of interspecific introgression lines for tomato improvement. *Nature Biotechnology* **24**, 447–454.

Schauer N, Semel Y, Balbo I, Steinfath M, Repsilber D, Selbig J, Pleban T, Zamir D, Fernie AR. 2008. Mode of inheritance of primary metabolic traits in tomato. *The Plant Cell* **20**, 509–523.

Schuster J, Binder S. 2005. The mitochondrial branched-chain amino transferase (AtBCAT1) is capable to initiate degradation of leucine, isoleucine and valine in almost all tissues of *Arabidopsis*. *Plant Molecular Biology* **57**, 241–254.

Schuster J, Knill T, Reichelt M, Gershenzon J, Binder S. 2010. BRANCHED-CHAIN AMINOTRANSFERASE4 is part of the chain elongation pathway in the biosynthesis of methionine-derived glucosinolates in *Arabidopsis*. *The Plant Cell* **18**, 2664–2679.

Sulpice R, Trenkamp S, Steinfath M, et al. 2010. Network analysis of enzyme activities and metabolite levels and their relationship to biomass in a large panel of *Arabidopsis* accessions. *The Plant Cell* **22**, 2872–2893.

Taylor NL, Heazlewood JL, Day DA, Millar AH. 2004. Lipoic acid-dependent oxidative catabolism of alpha-keto acids in mitochondria provides evidence for branched-chain amino acid catabolism in *Arabidopsis*. *Plant Physiology* **134**, 838–848.

Valle EM, Boggio SB, Heldt HW. 1998. Free amino acid composition of phloem sap and growing fruit of *Lycopersicon esculentum*. *Plant and Cell Physiology* **39**, 458–461.

Van der Hoeven R, Ronning C, Giovannoni J, Martin G, Tanksley S. 2002. Deductions about the number, organization, and evolution of genes in the tomato genome based on analysis of a large expressed sequence tag collection and selective genomic sequencing. *The Plant Cell* **14**, 1441–1456.

Walters DS, Steffens JC. 1990. Branched-chain amino acid metabolism in the biosynthesis of *Lycopersicon pennellii* glucose esters. *Plant Physiology* **93**, 1544–1551.

Zanor MI, Osorio S, Nunes-Nesi A, et al. 2009. RNA Interference of LIN5 in tomato confirms its role in controlling Brix content, uncovers the influence of sugars on the levels of fruit hormones, and demonstrates the importance of sucrose cleavage for normal fruit development and fertility. *Plant Physiology* **150**, 1204–1218.